Hindawi
Journal of Analytical Methods in Chemistry
Volume 2023, Article ID 8819534, 17 pages
https://doi.org/10.1155/2023/8819534

Research Article

Characterization of the Active Ingredient and Prediction of the Potential Mechanism of Dahuoluo Pill via Mass Spectrometry with the Network Pharmacology Method

Haoran Xu,[1] **Yuelin Bi**,[1] **Xin Feng**,[1] **Jiaqi Wang**,[1] **Gengyuan Yu**,[1] **Tonghua Zhang**,[1] **Tianyi Li**,[1] **Xuhua Gao**,[1] **Runhua Liu**,[1] **Yu Sun**,[1] **Hao Wu**,[1] **Linlin Fang**,[2] **Chenning Zhang**,[1,3] **and Yikun Sun**[1]

[1]*School of Chinese Materia Medica, Beijing University of Chinese Medicine, Beijing 102488, China*
[2]*College of Pharmacy, Dalian Medical University, Dalian, Liaoning 116044, China*
[3]*Department of Pharmacy, Xiangyang No. 1 People's Hospital, Hubei University of Medicine, Xiangyang 441100, China*

Correspondence should be addressed to Linlin Fang; fanglinlin880616@163.com, Chenning Zhang; zhangcn1118@163.com, and Yikun Sun; sunyk@bucm.edu.cn

Received 17 March 2023; Revised 21 September 2023; Accepted 11 October 2023; Published 7 November 2023

Academic Editor: Antony C. Calokerinos

The Dahuoluo pill (DHLP) is a classic Chinese patent medicine used to treat rheumatoid arthritis and other conditions. However, there has been no research on the chemical components of DHLP and the mechanisms by which it ameliorates rheumatoid arthritis. Hence, we analysed the chemical components of DHLP and the DHLP components absorbed in blood by using ultraperformance liquid chromatography-Q-exactive-orbitrap-mass spectrometry. We then used network pharmacology to predict the underlying mechanisms by which DHLP ameliorates rheumatoid arthritis. We identified 153 chemical compounds from DHLP, together with 27 prototype components absorbed in blood. We selected 48 of these compounds as potential active ingredients to explore the mechanism. These compounds are related to 88 significant pathways, which are linked to 18 core targets. This study preliminarily reveals the potential mechanisms by which DHLP ameliorates rheumatoid arthritis and provides a basis for further evaluation of the drug's efficacy.

1. Introduction

Rheumatoid arthritis (RA) is a chronic and systemic inflammatory disease with a prevalence ranging from 0.4% to 1.3% of the population, depending on sex (women are affected 2–3 times more often than men) and age (the frequency of new RA diagnoses peaks in the sixth decade of life) [1]. The cause of RA is still unknown. The main symptoms of this disease are pain and swelling in the joints of the hands or feet, which interfere with quality of life. These clinical manifestations of RA are stimulated by receptor activators of nuclear factor κB ligand (RANKL), tumour necrosis factor (TNF), and interleukin (IL)-6 [2]. Many drugs have been used to treat RA, including nonsteroidal anti-inflammatory drugs (NSAIDs), glucocorticoids, and disease-modifying antirheumatic drugs (DMARDs) [3]. In recent years, the use of traditional Chinese medicine (TCM) to treat RA has been effective and very popular with patients. TCM can avoid some adverse drug reactions, including infections, nausea, and vomiting, and is more suitable for long-term use [4].

The Dahuoluo pill (DHLP) is made from 50 ingredients, including *Cinnamomum cassia*, *Ephedra*, *Rhizoma coptidis,* and *Angelica sinensis*, which are collected in the *Medicine Standards of the Ministry of Health of People's Republic of China Traditional Chinese Medicine Prescriptions* (Volume

17). DHLP is widely used clinically for its effects of dispelling wind and dampness and relaxing muscles and collaterals, among others. As a famous Chinese patent medicine, the clinical application of DHLP is the treatment of cerebral infarction [5], frozen shoulder [6], and RA [7]. Modern experiments have proved that DHLP can promote peripheral vascular microcirculation, relax blood vessels, and relieve thrombosis [8]. The ingredients in DHLP, such as chlorogenic acid, ligustride I, and Z-ligustilide, have proven anti-inflammatory effects [9]. However, the mechanism by which DHLP ameliorates RA is not completely clear, and further exploration is required.

In recent years, network pharmacology has been widely used in TCM. The disease-gene-target-drug network is a common approach of network pharmacology, and the characteristics of integrity and comprehensiveness of network pharmacology are compatible with the feature of complex components, numerous targets, and diverse regulatory mechanisms in TCM. Therefore, we selected the main chemical components from DHLP as the active ingredients and employed network pharmacology to explore the mechanism by which DHLP ameliorates RA. In the current study, we used ultraperformance liquid chromatography-Q-exactive-orbitrap-mass spectrometry (UPLC-Q-exactive-orbitrap-MS) to identify the chemical components *in vitro* and the components from DHLP absorbed in rat plasma. Furthermore, we screened the main identified components to explore the target and mechanism of DHLP in the treatment of RA through network pharmacology. This experiment provides a new method for the quality control of DHLP and a theoretical basis for its development and utilisation.

2. Materials and Methods

2.1. Materials. Acetonitrile (MS grade) was supplied by China Thermo Fisher Scientific Co. Ltd. Formic acid (MS grade) was purchased from US ROE company. DHLP (lot no. 19013262) was obtained from Beijing Tongrentang Pharmaceutical Group Co. Ltd. Water was derived from a Milli-Q Ultrapure water purification system (Millipore, Bedford, MA, USA).

Six male Sprague–Dawley rats (300–320 g) were procured from Si Pei Fu Biotechnology Co. Ltd. (Beijing, China). The rats were divided into an experimental group and a normal group and housed in the experimental animal center of the Beijing University of Chinese Medicine (Beijing, China) at $23 \pm 2^{\circ}$C and $60\% \pm 5\%$ relative humidity, with access to water and a normal diet *ad libitum*. The animal experiment protocol was approved by the Animal Care and Use Committee of the Beijing University of Chinese Medicine.

2.2. Analysis of the DHLP Chemical Components In Vitro

2.2.1. Preparation of the Sample Solution. A portion of DHLP (3.5 g) was cut into small pieces and dissolved in 35 mL of 75% methanol at a ratio of 1 : 10. The stock solution was extracted by the heating reflux method for 1 h. The decoction liquid was centrifuged for 10 min at 12000 rpm and diluted five times, taking 5 μL of the diluent for MS analysis.

2.2.2. Chromatographic Conditions. An ACQUITY UPLC BEH C18 column (1.7 μm, 2.1 × 150 mm; Waters, Milford, MA, USA) was used, with a column temperature of 40°C, an injection volume of 5 μL, a flow rate of 0.3 mL/min, and a mobile phase containing 0.1% formic acid aqueous solution (A) and acetonitrile (B). The gradient elution program was as follows: 0–2 min, 5% B; 2–17 min, 5%–98% B; 17–19 min, 98% B; 19–23 min, 98%–5% B; and 23–25 min, 5% B.

2.2.3. MS Conditions. Electrospray ionisation (ESI) was used for the ion source, positive and negative ions were alternately scanned, the scan mode was a full scan/data-dependent two-stage scan (full scan/ddMS^2), the scan range was 100–1300 Da, and the capillary temperature was 350°C. The spray voltage in the positive mode was 3200 V, the spray voltage in the negative mode was 3800 V, the sheath gas was 35 arb, and the auxiliary gas was 15 arb. MS^2 uses three collision energies, low, medium, and high, to perform the second level of the precursor ion. The positive ion mode was 30, 40, and 50 V, and the negative ion mode was 30, 40, and 50 V. The resolution of the primary mass spectra was full scan 70000 full width at half maximum (FWHM), and the resolution of the secondary mass spectra was MS/MS17500 FWHM.

2.2.4. Compound Identification. The raw data were processed with Thermo Xcalibur Qual Browser 3.0.63, which could detect the mass, retention time, and intensity of the peaks in each chromatogram. The chemical components of DHLP were determined by comparison to the relevant data.

2.3. Analysis of Absorbed Components In Vivo

2.3.1. Drug Intervention. The DHLP sample was dissolved in distilled water. The three rats in the experimental group were given the suspension by intragastric administration at a dose of 10.33 g/kg (clinical five-fold measurement) twice a day for 3 days; the three rats in the normal group were given normal saline via intragastric administration twice a day for 3 days. After the last administration, 0.2 mL of blood was collected in a heparinised microcentrifuge tube from the tail vein at the following time points: 15 min, 30 min, 1 h, 2 h, 4 h, and 6 h. The samples were then centrifuged at 4000 rpm for 10 min, and the supernatant was frozen at −80°C until analysis.

2.3.2. Preparation of Plasma Samples. Plasma samples frozen at −80°C were thawed at room temperature. The plasma samples from different time points were mixed in equal amounts. Then, 360 μL of methanol solution was added to 120 μL of the mixed plasma sample, and the resulting sample was vortexed for 3 min, sonicated in an ice-filled ultrasonic

water bath for 10 min, and centrifuged at 4000 rpm for 10 min. The supernatant was removed and blow-dried at 40°C under nitrogen. The residue was dissolved in 100 μL of methanol, vortexed for 30 s, and centrifuged at 12000 rpm for 10 min. The injection volume was 5 μL.

2.3.3. Detection and Analysis. The samples were injected according to the above detection conditions. Qualitative analysis of the prototype composition in the plasma sample was based on the DHLP chemical composition identification results, combined with the retention time and fragment ion information.

2.4. Network Pharmacology

2.4.1. Screening of Active Ingredients. The identified compounds from the DHLP chromatogram with an m/z intensity of $>10^8$ kg/C were screened as the active ingredients. Meanwhile, to avoid ignoring highly recognised active ingredients, the Chinese Pharmacopoeia (2020 edition) and the relevant literature were used to obtain the ingredients. These findings were merged with the screening results from the ion current diagram. The SwissTargetPrediction website (https://www.swisstargetprediction.ch/) was used for target prediction.

2.4.2. Target Prediction of RA. The human Online Mendelian Inheritance in Man (OMIM, https://www.omim.org/) knowledge base and a human gene database (GeneCards, https://www.genecards.org/) were used to acquire disease targets by entering the keyword "rheumatoid arthritis."

2.4.3. Construction of the Protein-Protein Interaction (PPI) Network. A bioinformatics website (https://www.bioinformatics.com.cn/) was used to visualise the intersection between the component targets and the disease targets with a Venn diagram. The common targets were imported into the STRING website (https://string-db.org/) to draw the PPI network, and then, Cytoscape 3.7.1 was used to visualise the protein network structure and to analyse the topological characteristics. The medians of the three parameters of degree centrality (DC), betweenness centrality (BC), and closeness centrality (CC) were used as the screening condition. The core targets for the component treatment of RA were obtained by screening twice.

2.4.4. Gene Ontology (GO) Analysis and Kyoto Encyclopedia of Genes and Genomes (KEGG) Enrichment Analysis. The direct targets of the ingredients on RA were imported into the DAVID website (https://david.ncifcrf.gov/). GO and KEGG enrichment maps were made through a bioinformatics website (https://www.bioinformatics.com.cn/).

2.4.5. Network Construction. The TCM, components, targets, and pathways of DHLP were imported into Cytoscape 3.7.1 to establish a TCM-component-target-pathway network.

3. Results

3.1. Identification of the Chemical Constituents. Based on the optimised chromatographic and MS analysis conditions, we analysed the components of DHLP. We identified that 153 compounds were under the positive and negative ion modes, including 34 alkaloids, 27 flavonoids, 19 terpenes, 16 glycosides, and 10 phenylpropanoids. The base peak integration is shown in Figure 1. The classification diagrams of the identified compounds are shown in Figure 2. The chemical composition lists are shown in Table 1 for the negative ion mode and Table 2 for the positive ion mode.

3.1.1. Alkaloids. Hypaconitine is a terpene alkaloid, and the diagnostic ions related to it include $[M+H-CH_3OH]^+$, $[M+H-OCOCH_3]^+$, and $[M+H-OCOCH_3-CH_3OH]^+$. In the positive ion flow diagram, the retention time of peak 67 is 10.25 min, and its quasi-molecular ion peak is m/z 616.3111 $[M+H]^+$. The fragment ions coincide with that of hypaconitine, so we determined that the compound is hypaconitine. The cleavage law of hypaconitine and the secondary mass spectrum are shown in Figure 3(a).

Ephedrine is an organic amine alkaloid. The N atom in its side chain is relatively active, and the substituents attached to the N atom are easily lost by MS collisions. In the positive ion flow diagram, the retention time of peak 11 is 5.38 min, and its quasi-molecular ion peak is m/z 166.1227 $[M+H]^+$. At the same time, the characteristic fragments of m/z 148.1120 $[M+H-H_2O]^+$, $[M+H-H_2O-CH_3]^+$, and $[M+H-H_2O-NH_2CH_3]^+$ can be observed. Hence, we determined that the compound is ephedrine. The cleavage law of ephedrine and the secondary mass spectrum are shown in Figure 3(b).

Berberine is an isoquinoline alkaloid. It is prone to $[M+H-CH_3]^+$, and then, further removal of the H connected to N produces $[M+H-CH_4]^+$, which can remove CO at the same time to get $[M+H-CH_4-CO]^+$ and can also remove CH_2 to get $[M+H-CH_4-CH_2]^+$. The quasi-molecular ion peak and the fragment ions of compound 54 coincide with berberine. The cleavage law of berberine and the secondary mass spectrum are shown on the left side of Figure 3(c).

3.1.2. Flavonoids. Puerarin is an isoflavone, which mainly undergoes cleavage of the D ring-glycosidic bond, forming a stable conjugate between the A, B, and C rings, which is not easy to break. The pyrolysis characteristics of puerarin are m/z 399, 381, 363, 321, 297, and 279, which coincide with compound 22. The cleavage law of puerarin and the secondary mass spectrum are shown on the right side of Figure 3(d).

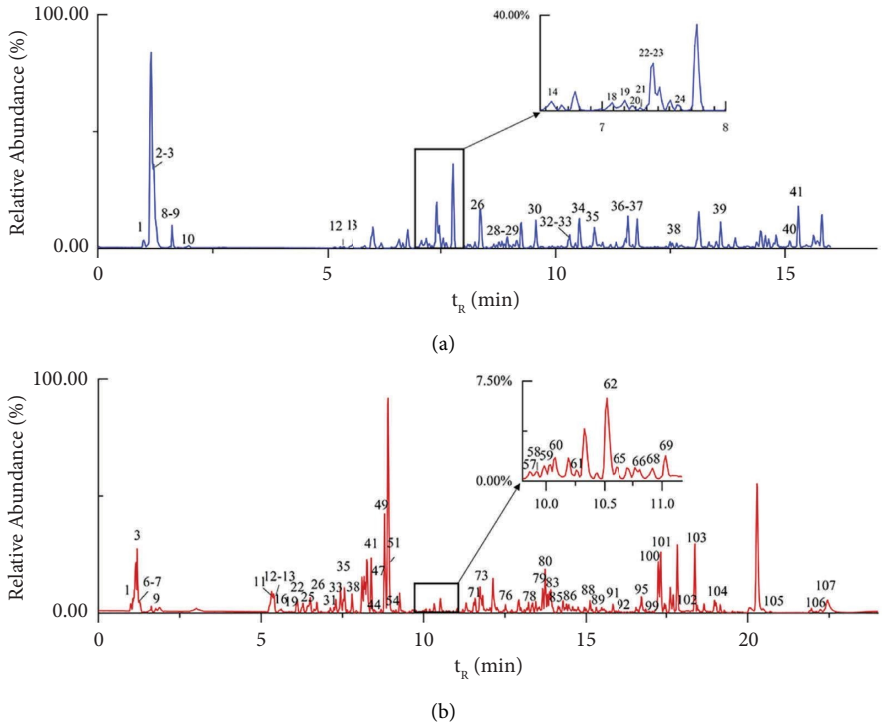

Figure 1: Base peak ion flow diagram of DHLP under negative ion (a) and positive ion (b) by UPLC-Q-exactive-orbitrap-MS.

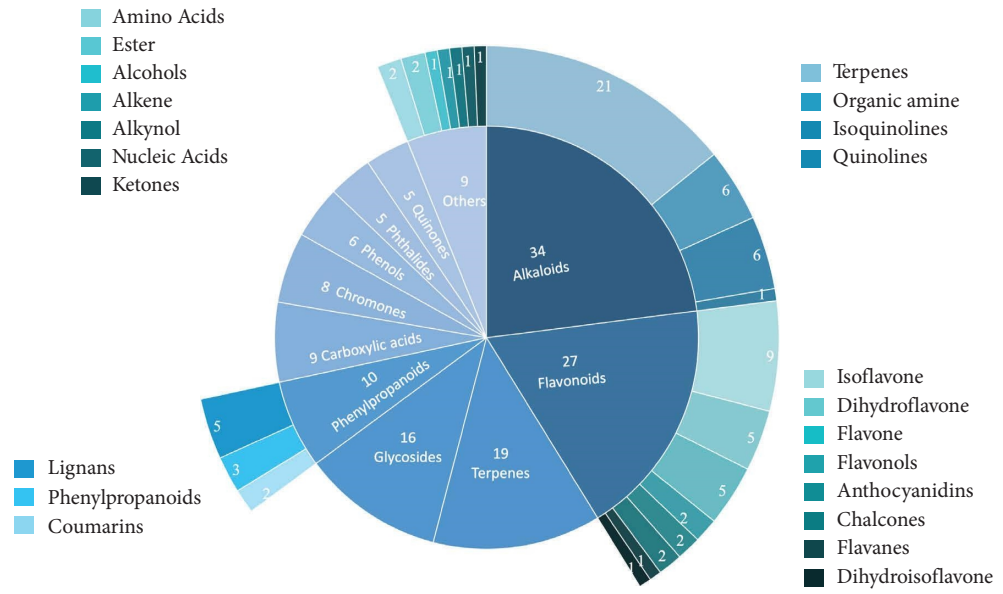

Figure 2: Compounds classified.

Baicalein is an isoflavone, and its cleavage characteristics are similar to that of puerarin. In the positive ion flow diagram, compound 59 coincides with baicalein, whose fragment ions include m/z 253.0493 $[M+H-H_2O]^+$, 241.0493 $[M+H-CO]^+$, 225.0544 $[M+H-H_2O-CO]^+$, and 195.0436 $[M+H-2CO-H_2O]^+$. At the same time, the compound can undergo an RDA reaction to generate the fragment ion m/z 169.0646. The cleavage law of baicalein and the secondary mass spectrum are shown on the left side of Figure 3(e).

Kaempferol is a flavonol, which loses CO through the cleavage of the C ring to produce m/z 257.0452 $[M-H-CO]^-$ (Table 3). Further loss of CO or H_2O produces m/z 229.0510 $[M-H-2CO]^-$ or 239.0349

Table 1: The identified chemical constituents in DHLP by UPLC-Q-exactive-orbitrap-MS under negative ion.

No.	t_R (min)	Measured value	MS/MS	Formula	Identification	Error (ppm)	Source
1	1.08	319.1520	167.0809; 139.0866; 137.0708; 123.0555; 109.0763	$C_{17}H_{18}O_6$	Evofolin B [10]	1.88	Cinnamomum cassia
2	1.21	493.1222	331.1624; 313.0565; 169.0134; 151.0029; 125.0234	$C_{19}H_{26}O_{15}$	Gallic acid-O-diglucoside [11]	−4.66	Rhubarb
3	1.22	191.0555	129.0181; 111.0077	$C_6H_8O_7$	Citric acid [12]	2.09	Radix polygoni multiflora/radix rehmanniae preparata
4	1.24	331.0679	211.0244; 169.0136; 125.0234	$C_{13}H_{16}O_{10}$	Glucogallin [13]	−2.42	Radix aconiti kusnezoffii
5	1.29	169.0135	125.0234; 150.9698	$C_7H_6O_5$	Gallic acid [12]	4.14	Radix polygoni multiflori
6	1.41	341.1083	179.0556; 135.0452	$C_{15}H_{18}O_9$	1-O-Caffeoyl glucoside [14]	−0.88	Rhizoma drynariae
7	1.49	191.0555	173.0083; 127.0386; 111.0076	$C_7H_{12}O_6$	Quinic acid [13]	3.14	Radix aconiti kusnezoffii
8	1.63	243.0634	111.0188; 68.0129	$C_9H_{12}N_2O_6$	Uridine [15]	−4.94	Radix rehmanniae preparata
9	1.64	331.0679	271.0461; 169.0135; 125.0234	$C_{13}H_{16}O_{10}$	Gallic acid-O-glucoside [11]	−2.42	Rhubarb
10	1.87	169.0135	125.0234	$C_7H_6O_5$	Gallic acid [13]	4.14	Radix aconiti kusnezoffii
11	3.85	153.0184	109.0284; 91.0177; 81.0333	$C_7H_6O_4$	Protocatechin [10]	5.88	Cinnamomum cassia
12	5.43	353.0880	191.0555	$C_{16}H_{18}O_9$	Chlorogenic acid [16]	−0.57	Ephedra/rhizoma coptidis/angelica sinensis
13	5.45	431.0991	311.0562; 269.0453; 265.0520; 225.0553	$C_{21}H_{20}O_{10}$	Anthraglycoside B [10]	−1.62	Cinnamomum cassia
14	6.19	289.1455	245.1552	$C_{15}H_{14}O_6$	Catechin [12]	1.38	Radix polygoni multiflori
15	6.30	207.0299	192.0423; 148.0522	$C_{11}H_{12}O_4$	Trans-3,4-dimethoxycinnamic acid [17]	0	Rhizoma coptidis
16	6.93	300.9990	283.9962; 257.0093	$C_{14}H_6O_8$	Ellagic acid [13]	0	Radix aconiti kusnezoffii/radix paeoniae rubra/myrrha
17	6.97	549.1635	255.0663; 135.0078	$C_{26}H_{30}O_{13}$	Celery glycyrrhizin [18]	−4.01	Glycyrrhiza uralensis
18	7.08	417.1196	255.0663; 135.0078	$C_{21}H_{22}O_9$	Liquiritin [18]	−1.19	Glycyrrhiza uralensis
19	7.14	405.0690	243.0661	$C_{20}H_{22}O_9$	2,3,5,4′-Tetrahydroxystilbene glucoside [12]	0.25	Radix polygoni multiflori
20	7.21	167.0342	123.0076	$C_8H_8O_4$	Vanillic acid [19]	4.79	Angelica sinensis
21	7.33	193.0500	179.0300; 149.0598	$C_{10}H_{10}O_4$	Ferulic acid [19]	3.11	Angelica sinensis
22	7.39	623.2018	461.1673; 161.0236	$C_{29}H_{36}O_{15}$	Acteoside [15]	4.65	Radix rehmanniae preparata
23	7.44	579.8508	459.1163; 271.0614; 151.0027	$C_{27}H_{32}O_{14}$	Naringin [14, 20, 21]	1.55	Qingpi/rhizoma drynariae
24	7.51	295.1198	173.0085	$C_{13}H_{12}O_8$	2-O-Caffeoylmalic acid [16]	−0.34	Ephedra
25	7.73	609.1401	301.0353	$C_{28}H_{34}O_{15}$	Hesperidin [22]	0.82	Qingpi
26	8.38	631.9897	193.0500; 175.0394	$C_{31}H_{40}O_{15}$	Rehmaionoside/isomartynoside [15]	−0.46	Radix rehmanniae preparata
27	8.63	253.0506	225.0561	$C_{15}H_{10}O_4$	Chrysophanic acid [23]	0	Rhubarb
28	8.65	447.0940	285.0406	$C_{22}H_{24}O_{10}$	2,3,5,4′-Tetrahydroxystilbene-2-O-acetyl-glucoside [12]	−0.89	Radix polygoni multiflori
29	8.82	255.0664	153.0185; 135.0185; 119.0492	$C_{15}H_{12}O_4$	Isoliquiritigenin [18]	−1.57	Glycyrrhiza uralensis
30	8.89	285.0411	257.0452; 239.0349; 229.0510; 151.0027	$C_{15}H_{10}O_6$	Kaempferol [24]	−2.11	Glycyrrhiza uralensis/rhizoma drynariae/ephedra
30	9.61	837.3923	661.3602; 485.3271; 351.0572	$C_{42}H_{62}O_{17}$	Licoricesaponin G2 [18]	−1.07	Glycyrrhiza uralensis
32	10.29	269.0458	241; 0508; 225.0550	$C_{15}H_{10}O_5$	Aloe-emodin [23]	−1.12	Rhubarb
33	10.34	299.0570	284.0327	$C_{16}H_{12}O_6$	Kaempferide [24]	−3.01	Clove
34	10.49	821.3983	645.3605; 469.3316; 351.0573; 193.0349; 113.0233	$C_{42}H_{62}O_{16}$	Glycyrrhizic acid [18]	−2.19	Glycyrrhiza uralensis

Table 1: Continued.

No.	t_R (min)	Measured value	MS/MS	Formula	Identification	Error (ppm)	Source
35	10.96	807.4189	351.0571; 193.0350.113.0233	$C_{42}H_{64}O_{15}$	Glycyrrhizin B2 [18]	−2.11	Glycyrrhiza uralensis
36	11.54	283.0255	239.0349; 183.0445	$C_{15}H_8O_6$	Rheinic acid [23]	−2.47	Rhubarb
37	11.62	327.1241	177.0915; 165.0549; 147.0802	$C_{15}H_{20}O_8$	Dihydromelilotoside [10]	2.14	Cinnamomum cassia
38	12.53	371.1506	193.0867; 177.0192; 163.0400; 123.0441	$C_{20}H_{20}O_7$	Glycosmisic acid [10]	−2.42	Cinnamomum cassia
39	13.50	351.0878	307.0975; 237.0918	$C_{20}H_{32}O_5$	Cinncassiol D4 [10]	−1.14	Cinnamomum cassia
40	15.18	435.1436	417.133	$C_{21}H_{22}O_{10}$	Dihydro kaempferol-7-O-rhamnoside [14]	−3.68	Rhizoma drynariae
41	15.34	283.0614	240.0427	$C_{16}H_{12}O_5$	Emodin monomethyl ether [23]	−0.71	Rhubarb

Table 2: The identified chemical constituents in DHLP by UPLC-Q-exactive-orbitrap-MS under positive ion.

No.	t_R (min)	Measured value	MS/MS	Formula	Identification	Error (ppm)	Source
1	1.07	175.1188	158.0922; 130.0974; 116.0704; 70.0657	$C_6H_{14}N_4O_2$	Arginine [24]	0.57	Rhizoma arisaematis
2	1.14	295.0961	277.1029; 259.0919; 241.0819; 211.0710	$C_{18}H_{14}O_4$	Isoimperatorin [25]	1.36	Saposhnikovia divaricata
3	1.15	127.0389	109.0285	$C_6H_6O_3$	5-Hydroxymethyl-2-furaldehyde [19]	1.57	Angelica sinensis
4	1.16	145.0494	127.0389; 109.0287	$C_6H_8O_4$	Pyranone [26]	1.38	Glycyrrhiza uralensis
5	1.22	305.1015	287.1230; 273.1275	$C_{16}H_{16}O_6$	Hesperetin dihydrochalcone [24]	1.64	Clove
6	1.23	280.1390	262.1281	$C_{11}H_{21}NO_7$	N-Fructosyl valine [24]	0.36	Rhizoma arisaematis
7	1.24	256.0724	147.0442	$C_{15}H_{12}O_4$	Liquiritigenin [16]	4.69	Glycyrrhiza uralensis
8	1.28	230.1531	166.0857; 145.0491; 128.1065	$C_{15}H_{19}ON$	Atractylenolactam [22]	3.48	Atractylodes macrocephala koidz
9	1.82	121.0648	105.0449; 93.0702	C_8H_8O	1-Acetophenone [19]	0	Angelica sinensis
10	3.62	394.2514	376.2479; 358.2379	$C_{22}H_{35}NO_5$	Karakolidine [13]	−1.01	Radix aconiti kusnezoffii
11	5.38	166.1262	148.1120; 133.0887; 117.0701	$C_{10}H_{15}NO$	Ephedrine/pseudoephedrine [26]	1.20	Ephedra
12	5.38	148.1120	133.0887	$C_{10}H_{13}N$	5,6,7,8-Tetrahydro-4-methylquinoline [26]	0.68	Ephedra
13	5.48	408.2646	390.2631	$C_{23}H_{37}NO_5$	Isotalatizidine [13]	4.90	Radix aconiti kusnezoffii
14	5.49	378.2634	360.2529	$C_{22}H_{35}NO_4$	Carmichaeline [27]	1.32	Aconitum carmichaelii debx
15	5.59	355.2476	337.0915; 319.0813; 301.0712	$C_{20}H_{34}O_5$	Incensole trioxide [19]	0.84	Frankincense
16	5.62	360.2437	342.2431	$C_{22}H_{33}NO_3$	Napelline [13]	5.00	Radix aconiti kusnezoffii
17	5.64	180.1382	162.1276; 147.1041; 132.0813	$C_{11}H_{17}NO$	Mephedrone [26]	0.56	Ephedra
18	5.66	408.2745	390.2631	$C_{23}H_{37}NO_5$	Talatizidine [27]	−0.24	Aconitum carmichaelii debx
19	5.73	193.0494	161.0596; 133.0648; 149.0589; 105.0702	$C_{10}H_8O_4$	Scopoletin [25]	0.52	Saposhnikovia divaricata
20	5.81	358.2372	340.2267	$C_{22}H_{31}NO_3$	Songorine [13, 25]	1.40	Aconitum carmichaelii debx/ radix aconiti kusnezoffii
21	5.95	355.1533	337.0915; 319.0809	$C_{21}H_{22}O_5$	14-Acetyl-kirilightacyl-12-transtractylodes triol [21]	1.97	Atractylodes macrocephala koidz
22	6.06	417.1176	399.1070; 381.0966; 351.0860	$C_{21}H_{20}O_9$	Puerarin [17]	0.96	Radix puerariae
23	6.19	454.2795	436.2694; 404.2429	$C_{24}H_{39}NO_7$	Fuziline [13, 25]	0.88	Aconitum carmichaelii debx/ radix aconiti kusnezoffii
24	6.26	447.1281	429.1180; 411.1072; 393.0968	$C_{22}H_{22}O_{10}$	Oxyayanin b trimethyl ether [17]	1.12	Radix puerariae
25	6.41	438.2542	420.2742; 388.2481	$C_{24}H_{39}NO_6$	Neoline [13, 25]	1.83	Aconitum carmichaelii debx/ radix aconiti kusnezoffii
26	6.60	417.1183	255.0649	$C_{21}H_{20}O_9$	Daidzin [17]	−0.72	Radix puerariae
27	6.77	422.2836	390.2633	$C_{24}H_{39}NO_5$	Talatizamine [13]	−3.08	Radix aconiti kusnezoffii
28	6.95	344.2508	326.2475	$C_{22}H_{33}NO_2$	Bullatine A [13]	−0.58	Radix aconiti kusnezoffii
29	7.05	549.1598	531.1501; 513.1383; 495.1281; 411.1072; 393.0967; 375.0859	$C_{26}H_{28}O_{13}$	Chrysin-6-C-arabinose-8-C-glucoside [28]	0.91	Radix scutellariae
30	7.16	163.0389	135.0441; 117.0337; 105.0704; 89.0390	$C_9H_6O_3$	Umbelliferone [25]	0.61	Saposhnikovia divaricata
31	7.20	286.1434	269.1169; 239.0707; 237.0909; 209.0961; 194.0724; 143.0491; 115.0544	$C_{17}H_{19}NO_3$	Coclaurine [29]	1.40	Radix linderae

Table 2: Continued.

No.	t_R (min)	Measured value	MS/MS	Formula	Identification	Error (ppm)	Source
32	7.20	463.0861	287.0546	$C_{21}H_{18}O_{12}$	5,7-dihydroxyl-2′-methoxyflavone-7-O-Gluconaldehyde [28]	2.16	Radix scutellariae
33	7.20	208.0966	165.0909; 150.0678	$C_{11}H_{13}NO_3$	Thalietrine [17]	0.96	Rhizoma coptidis
34	7.23	245.1170	227.0700; 199.0752; 141.0696; 128.0624; 115.8399; 91.0546	$C_{15}H_{16}O_3$	Linderalactone [29]	0.82	Radix linderae
35	7.27	319.1172	301.1067; 283.0962; 255.1013; 227.1065; 164.0467	$C_{17}H_{18}O_6$	Agarotetrol [30]	1.25	Aquilaria agallocha
36	7.49	581.1868	435.1288; 273.0755; 153.0182	$C_{27}H_{32}O_{14}$	Naringenin [14]	−0.52	Rhizoma drynariae
37	7.54	453.1750	291.1222; 273.1117; 259.0960; 243.0649; 219.0649; 205.0494	C22H28O10	5-O-Methylvisammioside [31]	1.10	Saposhnikovia divaricata
38	7.57	319.1169	301.1065; 283.0960; 255.1012; 227.1063; 164.0466	$C_{17}H_{18}O_7$	Aquilarone B [30]	2.19	Aquilaria agallocha
39	7.65	317.0653	302.0419; 285.0396	$C_{16}H_{12}O_7$	Rhamnetin/isorhamnetin [24]	0.95	Clove
40	7.80	611.1964	449.1447; 413.1447; 431.1324; 369.0963; 345.0966; 303.0859; 263.0545	$C_{28}H_{34}O_{15}$	Neohesperidin [32, 33]	0.98	Qingpi
41	7.95	477.1024	301.0703; 286.0468	$C_{22}H_{20}O_{12}$	5,7,2′-trihydroxy-6-methoxyflavone-7-O-glucuraldehyde glycosides [28]	0.63	Radix scutellariae
42	8.28	419.1335	257.0806; 239.0702; 229.0858	$C_{21}H_{22}O_9$	Liquiritin [26]	0.48	Glycyrrhiza uralensis
43	8.28	419.1720	223.9430; 211.0752	$C_{22}H_{26}O_8$	Flavaspidic acid ab [34]	−4.77	Guanzhong
44	8.31	339.1454	323.1136; 294.1117	$C_{20}H_{20}NO_4$	Jatrorrhizine [17]	3.24	Rhizoma coptidis
45	8.33	590.2904	572.2814; 540.2599; 508.2399	$C_{31}H_{43}NO_{10}$	14-benzoylmesaconine [13]	−3.90	Radix aconiti kusnezoffii
46	8.37	271.0598	253.0493; 243.0549	$C_{15}H_{10}O_5$	7,8,4′-Trihydroxyisoflavone [17]	1.11	Radix puerariae
47	8.49	447.0930	271.0598; 253.0494	$C_{21}H_{18}O_{11}$	Baicalin [28]	−1.79	Radix scutellariae
48	8.50	431.1340	269.0805	$C_{22}H_{22}O_9$	Ononin [17]	−0.93	Radix puerariae/Glycyrrhiza uralensis
49	8.51	269.0434	241.0492	$C_{15}H_8O_5$	Coumestrol [17]	3.72	Radix puerariae
50	8.69	604.3008	586.3019; 572.2835; 554.2741; 540.2741; 522.2476	$C_{32}H_{45}NO_{10}$	14-Benzoylaconine [13]	4.96	Radix aconiti kusnezoffii
51	8.69	255.0647	237.0543; 227.0699; 199.0751	$C_{15}H_{10}O_4$	Daidzein [17]	1.96	Radix puerariae
52	8.72	193.1221	175.0753; 147.0441	$C_{12}H_{16}O_2$	4-*n*-Pentylbenzoic acid [24]	1.04	Rhizoma arisaematis
53	8.84	291.1222	273.1118; 259.0953; 243.0649; 219.0649	$C_{16}H_{18}O_5$	5-O-Methylvisamminol [31]	−3.26	Saposhnikovia divaricata
54	8.88	337.1239	321.0967; 320.0914; 292.0970	$C_{20}H_{18}NO_4$	Berberine [17]	1.72	Rhizoma coptidis
55	8.95	461.1071	285.0752; 270.0518	$C_{22}H_{20}O_{11}$	Wogonoside [28]	1.52	Radix scutellariae
56	8.96	574.2904	542.2746; 510.2484	$C_{31}H_{43}NO_9$	14-Benzoylhypacoine [13]	4.88	Radix aconiti kusnezoffii
57	9.11	572.2804	554.2769; 540.2573; 522.2494	$C_{31}H_{41}NO_9$	Dehydrated benzoylmesacoine [13]	−4.89	Radix aconiti kusnezoffii
58	9.11	572.3168	540.2573; 508.2308	$C_{32}H_{45}NO_8$	14-O-Anisoylneoline [13]	−4.89	Radix aconiti kusnezoffii
59	9.12	203.1268	185.1328; 175.0387; 157.1009	$C_{10}H_{18}O_4$	Sebacic acid [24]	4.92	Rhizoma arisaematis
60	9.13	271.0598	253.0493; 241.0493; 225.0544; 197.0956; 169.0646	$C_{15}H_{10}O_5$	Baicalein [28]	1.11	Radix scutellariae
61	9.35	323.1136	294.0876	$C_{19}H_{16}NO_4$	Berberrubine [17]	4.95	Rhizoma coptidis
62	9.37	588.3069	556.2897; 524.2624	$C_{32}H_{45}NO_9$	14-benzoyl-methoxy-hypaconine [13]	3.40	Radix aconiti kusnezoffii

Table 2: Continued.

No.	t_R (min)	Measured value	MS/MS	Formula	Identification	Error (ppm)	Source
63	9.88	285.0753	270.0518; 267.0646; 257.0796	$C_{16}H_{12}O_5$	3′-Methoxyldaidzein [17]	1.40	Radix puerariae
64	9.95	327.1222	221.0806; 107.0494	$C_{19}H_{18}O_6$	Qinanone g (isomer) 2 [30]	1.53	Aquilaria agallocha
65	9.97	283.0960	192.0414; 164.0468	$C_{17}H_{14}O_4$	6,8-Dihydroxyl-2-(2-phenethyl) chromone [30]	1.41	Aquilaria agallocha
66	10.10	233.1534	215.1428; 187.1479; 159.1167; 145.1011; 131.0855	$C_{15}H_{20}O_2$	Costunolide [30]	0.86	Radix aucklandiae
67	10.25	616.3111	556.2897; 524.2632; 584.2874; 496.2664	$C_{33}H_{45}NO_{10}$	Hypaconitine [13]	0.81	Radix aconiti kusnezoffii
68	10.50	471.3462	407.3319; 121.1012	$C_{30}H_{46}O_4$	1-Carbonyl-β-boswellic acid [35]	1.49	Frankincense
69	10.68	327.1222	221.0807; 107.0484	$C_{19}H_{18}O_5$	Inanone g (isomer 1) [19]	1.53	Aquilaria agallocha
70	10.69	267.1014	252.0428; 224.0479	$C_{17}H_{14}O_3$	Dracorhodin [36]	4.87	Resina draconis
71	10.72	403.1380	388.1140; 373.0912; 355.0816; 327.0856	$C_{21}H_{22}O_8$	Nobiletin [32, 33]	1.74	Qingpi
72	10.80	217.0493	202.0259; 189.0905; 174.0310; 161.0594; 146.0358	$C_{12}H_8O_4$	Xanthotoxin [25]	0.92	Saposhnikovia divaricata
73	10.90	189.0909	161.0958; 147.0440; 130.0776; 119.0492; 105.0337	$C_{12}H_{12}O_2$	Z-Butylidenephthalide [19]	0.53	Angelica sinensis
74	10.94	249.1484	231.1373; 213.1272; 203.9383; 189.1274; 163.0751; 135.0803	$C_{15}H_{20}O_3$	Atractylenolide III [22]	4.42	Atractylodes macrocephala koidz
75	11.00	267.1010	176.0467; 161.0969; 137.0229	$C_{17}H_{14}O_3$	7-Hydroxyl-2-(2-phenethyl) chromone [30]	2.25	Aquilaria agallocha
76	11.00	323.2576	305.2469; 287.2367; 269.2253	$C_{20}H_{34}O_3$	Incensole oxide [19]	1.55	Frankincense
77	11.46	479.1162	317.1378; 299.6608	$C_{22}H_{22}O_{12}$	Isorhamnetin-3-O-glucoside [24]	4.59	Clove
78	11.52	285.0753	270.0518	$C_{16}H_{12}O_5$	Wogonin [28]	1.40	Radix scutellariae
79	11.77	352.1172	337.0939; 308.0923	$C_{20}H_{17}NO_5$	8-O-Berberine [17]	1.99	Rhizoma coptidis
80	11.80	257.0804	239.0698; 229.2530	$C_{15}H_{12}O_4$	Liquiritigenin [26]	1.17	Glycyrrhiza uralensis
81	11.92	203.0709	174.0316; 145.0287	$C_{12}H_{12}O_3$	3-butenyl-7-hydroxyphthalide [19]	2.46	Angelica sinensis
82	11.95	567.2014	549.1899; 531.1796; 283.0959; 267.1010; 255.1012; 239.1062	$C_{34}H_{30}O_8$	AH13 [30]	−0.18	Aquilaria agallocha
83	12.43	355.1040	191.0337; 161.0598	$C_{16}H_{18}O_9$	Chlorogenic acid [17]	−4.79	Rhizoma coptidis
84	12.63	194.1167	177.0898; 151.0627; 135.0439; 91.0544	$C_{11}H_{15}NO_2$	Racsalsoline [29]	4.64	Radix linderae
85	13.37	475.1534	371.0909; 341.0806	$C_{31}H_{23}O_5$	Nordacorubin [37]	1.26	Resina draconis
86	13.62	233.1537	215.1429; 187.1480; 151.0753	$C_{15}H_{20}O_2$	Atractylodes lactone II [21]	−0.43	Atractylodes macrocephala koidz
87	13.85	189.0909	171.1165; 159.0801; 131.0854	$C_{12}H_{12}O_2$	Butylidenephthalide [19]	0.53	Angelica sinensis
88	13.89	195.0650	178.0774; 148.9767	$C_{10}H_{10}O_4$	Ferulic acid [24]	1.03	Rhizoma arisaematis/clove
89	13.95	225.1118	207.1014; 151.0392	$C_{12}H_{16}O_4$	Chuanxionglide II [19]	1.33	Angelica sinensis
90	13.97	217.1584	157.1010; 147.1165; 143.0854; 131.0853; 129.0699; 121.0648; 119.0856	$C_{15}H_{20}O$	Atractylone [21]	1.38	Atractylodes macrocephala koidz
91	13.98	231.1378	213.1271; 195.1166; 185.1323; 171.0797	$C_{15}H_{18}O_2$	Atractylenolide I [21]	0.43	Atractylodes macrocephala koidz
92	14.33	231.1378	213.1272; 185.1325; 157.1011; 143.0855; 129.0694	$C_{15}H_{18}O_2$	Dehydrocostus lactone [30]	0.43	Radix aucklandiae

Table 2: Continued.

No.	t_R (min)	Measured value	MS/MS	Formula	Identification	Error (ppm)	Source
93	14.33	231.1378	213.1272; 195.1168; 185.1325; 155.0932; 141.0698; 128.0622	$C_{15}H_{18}O_2$	Linderenol [29]	0.87	Radix linderae
94	14.57	279.1215	261.2212; 243.2105; 173.1323; 109.1014; 91.0547	$C_{15}H_{18}O_5$	Aconitine A [29]	4.3	Radix linderae
95	14.57	279.2315	261.2212	$C_{18}H_{30}O_2$	γ-Linolenic acid [14]	1.07	Rhizoma drynariae
96	14.72	301.0704	286.1941	$C_{16}H_{12}O_6$	Baicalein II [28]	1.00	Radix scutellariae
97	15.27	381.2045	335.2005; 191.1065	$C_{24}H_{28}O_4$	Senkyunolide P [19]	3.93	Angelica sinensis
98	15.44	191.1065	173.0960; 145.1011; 117.0700; 105.0701; 91.0546	$C_{12}H_{14}O_2$	Z-Ligustilide [19]	0.52	Angelica sinensis
99	15.45	381.2048	363.1941; 335.1997; 293.1533	$C_{24}H_{28}O_5$	Eugelatinolide A [19]	3.15	Angelica sinensis
100	15.82	261.1120	243.2104; 215.1794; 173.1325; 145.1012; 129.0702; 105.0703; 91.0545	$C_{15}H_{16}O_4$	Isolinderalactone [29]	0.38	Radix linderae
101	15.98	499.3768	121.0649	$C_{32}H_{50}O_4$	Acetyl β-lactic acid [35]	2.80	Frankincense
102	16.46	852.5253	572.2840; 540.2577; 512.2659; 354.1691	$C_{49}H_{73}NO_{11}$	8-Linoleic acid-benzoylmesaconine [13]	0.35	Radix aconiti kusnezoffii
103	16.59	866.5411	586.2986; 526.2831; 494.2518	$C_{50}H_{75}NO_{11}$	8-Linoleic acid-benzoylaconine [13]	0.23	Radix aconiti kusnezoffii
104	16.62	836.5302	556.2900; 524.2636	$C_{49}H_{73}NO_{10}$	8-linoleic acid-benzoylhepaconine [13]	0.60	Radix aconiti kusnezoffii
105	16.88	828.5244	572.2844; 540.2590; 512.2673	$C_{47}H_{73}NO_{11}$	8-palmitic acid-benzoylmesaconine [13]	1.45	Radix aconiti kusnezoffii
106	16.93	365.2678	347.2577; 305.2469; 287.2365; 269.2263	$C_{22}H_{36}O_4$	Incensole oxide acetate [19]	2.19	Frankincense
107	17.04	812.5305	556.2896; 524.2642; 496.2780	$C_{47}H_{73}NO_{10}$	8-palmitic acid-benzoylhepaconine [13]	0.25	Radix aconiti kusnezoffii
108	17.2	513.3556	495.3528; 453.3362; 435.3258; 407.3304	$C_{32}H_{48}O_5$	3-Acetyl-11-ketone-β-mastic acids [19]	3.51	Frankincense
109	17.24	135.0804	105.0701; 91.0546; 79.0548	$C_9H_{10}O$	Cinnamic alcohol [10]	0	Cinnamomum cassia presl
110	17.26	307.2625	289.2519; 271.2418; 215.1787; 201.1635	$C_{20}H_{34}O_2$	Incensole [19]	1.95	Frankincense
111	17.26	307.1172	289.2519; 221.1909; 205.1953; 177.1638	$C_{16}H_{18}O_6$	Cimifugin [25]	1.30	Saposhnikovia divaricata
112	18.10	581.1868	563.3374; 545.3251	$C_{27}H_{32}O_{14}$	Naringin [32, 33]	−0.52	Qingpi
113	18.43	497.3615	437.3409; 409.3513; 391.3358	$C_{32}H_{48}O_4$	3α-acetyl-9,11Deoxidizing-β-boswellic acid [19]	2.01	Frankincense
114	18.94	457.3673	421.3467; 407.2956	$C_{30}H_{48}O_3$	β-Boswellic acid [35]	0.66	Frankincense
115	20.76	273.2571	229.4793; 217.1954; 163.1483; 149.1324	$C_{20}H_{32}$	Cupressene [19]	2.20	Frankincense
116	22.47	152.1064	133.9745; 116.9721	$C_9H_{13}NO$	Norephedrine [16]	3.94	Ephedra
117	22.65	152.1075	133.9798; 116.9721	$C_9H_{14}NO$	Pseudodesmethylephedrine [16]	−3.29	Ephedra

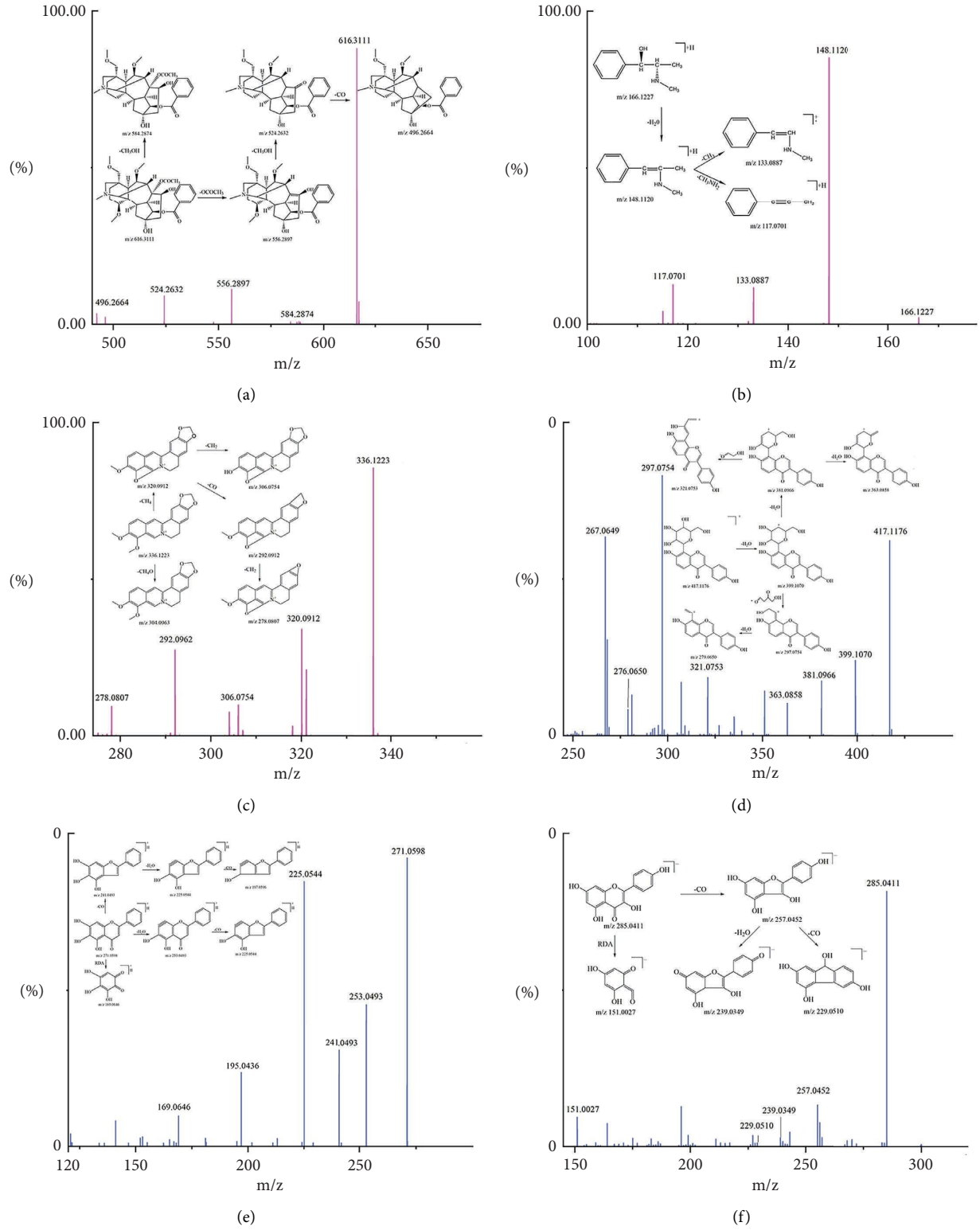

Figure 3: The MS/MS spectrums of alkaloids and flavonoids in positive ion mode or negative ion mode and their probable fragmentation pathway: (a) hypaconitine, (b) ephedrine, (c) berberine, (d) puerarin, (e) baicalin, and (f) kaempferol.

Table 3: The identified compounds absorbed into blood in DHLP by UPLC-Q-exactive-orbitrap-MS.

No.	Ion form	t_R (min)	Measured value	MS/MS	Formula	Identification	Error (ppm)	Type	Form (prototypes/metabolites)
1	$[M+H]^+$	1.08	175.1185	158.0920, 130.0972, 116.0705	$C_6H_{14}N_4O_2$	Arginine	−2.28	Amino acids	Prototypes
2	$[M-H]^-$	1.22	191.0191	129.0181, 111.0075	$C_6H_8O_7$	Citric acid	−3.14	Carboxylic acids	Prototypes
3	$[M-H]^-$	1.49	191.0555	173.0081, 121.6582, 111.0075	$C_7H_{12}O_6$	Quinic acid	−3.14	Phenols	Prototypes
4	$[M+H]^+$	2.38	127.0389	109.0285	$C_6H_6O_3$	5-Hydroxymethyl-2-furaldehyde	−1.57	Furans	Metabolites
5	$[M+H]^+$	5.03	148.1118	133.0885	$C_{10}H_{13}N$	5,6,7,8-Tetrahydro-4-methylquinoline	−2.03	Alkaloids	Metabolites
6	$[M-H]^-$	5.41	353.0876	191.0345	$C_{16}H_{18}O_9$	Chlorogenic acid	−0.57	Carboxylic acids	Prototypes
7	$[M+H]^+$	5.94	417.1172	399.1086, 381.0962, 351.0851	$C_{21}H_{20}O_9$	Puerarin	−1.92	Flavonoids	Prototypes
8	$[M-H]^-$	6.99	549.1628	255.0664, 135.0077	$C_{26}H_{30}O_{13}$	Celery glycyrrhizin	2.73	Flavonoids	Prototypes
9	$[M-H]^-$	7.07	417.119	255.0662, 135.0076	$C_{21}H_{22}O_9$	Liquiritin	−0.24	Flavonoids	Prototypes
10	$[M-H]^-$	7.38	579.1721	459.1163, 271.0614, 151.0027	$C_{27}H_{32}O_{14}$	Naringin	0.35	Glycosides	Prototypes
11	$[M+H]^+$	7.5	453.1744	291.1217, 273.1113, 259.0956, 243.0646, 219.0645, 205.0493	$C_{22}H_{28}O_{10}$	5-O-Methylvisammioside	−2.43	Glycosides	Prototypes
12	$[M+H]^+$	7.51	319.1147	301.1055, 283.0996, 255.1003, 227.1056, 164.0462	$C_{17}H_{18}O_7$	Aquilarone B	−9.09	Chromones	Prototypes
13	$[M-H]^-$	7.7	609.1824	301.0718	$C_{28}H_{34}O_{15}$	Hesperidin	−0.16	Glycosides	Prototypes
14	$[M-H]^-$	7.74	289.0713	245.1544	$C_{15}H_{14}O_6$	Catechin	−1.73	Flavonoids	Prototypes
15	$[M+H]^+$	8.28	271.0596	253.1943, 243.2106	$C_{15}H_{10}O_5$	7,8,4′-Trihydroxyisoflavone	−1.84	Flavonoids	Metabolites
16	$[M+H]^+$	8.28	271.0596	253.0493, 243.0549	$C_{15}H_{10}O_5$	7,8,4′-Trihydroxyisoflavone	−1.84	Flavonoids	Metabolites
17	$[M+H]^+$	8.56	255.0645	237.0537, 227.0698, 199.0749	$C_{15}H_{10}O_4$	Daidzein	−2.74	Flavonoids	Prototypes
18	$[M-H]^-$	8.57	253.0506	225.0547	$C_{15}H_{10}O_4$	Chrysophanic acid	0.40	Quinones	Prototypes
19	$[M+H]^+$	8.89	461.1069	285.0749, 270.0515	$C_{22}H_{20}O_{11}$	Wogonoside	−1.95	Flavonoids	Prototypes
20	$[M+H]^+$	9.5	271.0596	253.0493, 241.0493, 225.0544, 197.0956, 169.0646	$C_{15}H_{10}O_5$	Baicalein	−1.84	Flavonoids	Prototypes
21	$[M+H]^+$	9.82	285.0748	270.0520, 267.0643, 257.0804	$C_{16}H_{12}O_5$	3′-Methoxyldaidzein	−3.16	Flavonoids	Metabolites
22	$[M+H]^+$	10.08	233.1523	215.1419, 187.1477, 159.1165, 145.1009, 131.0854	$C_{15}H_{20}O_2$	Costunolide	−5.58	Terpenes	Prototypes
23	$[M-H]^-$	10.47	821.3971	351.0568	$C_{42}H_{62}O_{16}$	Glycyrrhizic acid	0.73	Saponosides	Prototypes
24	$[M-H]^-$	11.42	283.0247	239.0346, 183.0443	$C_{15}H_8O_6$	Rheinic acid	−0.35	Quinones	Prototypes
25	$[M+H]^+$	11.44	285.0748	270.0514	$C_{16}H_{12}O_5$	Wogonin	−3.16	Flavonoids	Prototypes
26	$[M-H]^-$	12.44	371.1132	193.0500, 177.0916	$C_{20}H_{20}O_7$	Glycosmisic acid	−1.08	Phenylpropanoids	Prototypes
27	$[M+H]^+$	13.97	225.1118	207.1012, 151.0389	$C_{12}H_{16}O_4$	Chuanxionglide II	−1.33	Ester	Prototypes

$[M - H - CO - H_2O]^-$, respectively. It also can undergo an RDA reaction to generate fragment ion m/z 151.0027. The cleavage law of kaempferol and the secondary mass spectrum are shown on the right side of Figure 3(f).

3.2. Network Pharmacology

3.2.1. Chemical Composition Screening and Target Prediction. We selected a total of 48 compounds: 36 of the identified compounds with the intensity $>10^8$ from the DHLP chromatogram and 12 compounds from the Chinese Pharmacopoeia (2020 edition) and the related literature. We used the SwissTargetPrediction website (https://www.swisstargetprediction.ch/) to predict targets, thereby obtaining a total of 1480 targets.

3.2.2. Target Prediction for RA. We found 1196 disease targets after searching the OMIM and GeneCards databases with "rheumatoid arthritis" as a keyword, and then screening, merging, and removing duplicates (Figure 4).

3.2.3. Construction of the PPI Network. We generated the Venn diagram through the bioinformatics website (Figure 5(a)). There are 167 common targets.

The STRING website is a functional protein association network that can predict PPIs. After importing all the targets into the website, we obtained and saved the PPI network in TSV format. We used Cytoscape 3.7.1 to analyse the topological characteristics of the protein network structure and to screen the core targets of the components for the treatment of diseases, as shown in Figure 5(b) and Table 4. The middle and innermost targets in Figure 5(b) are the results after the first screening, while the innermost layer is the result of the second screening. This later shows the core targets, sorted by the degree value from deep to shallow and from large to small. After sorting the 18 core targets, we found that AKT1 (degree = 52), MAPK1 (degree = 50), STAT3 (degree = 50), VEGFA (degree = 48), MAPK8 (degree = 45), EGFR (degree = 44), and TNF (degree = 43) are the key targets in this network.

3.2.4. GO Analysis and KEGG Enrichment Analysis. With a false discovery rate (FDR) <0.001 as the screening condition, we obtained 82 GO biological items, including response to the drug, response to lipopolysaccharide, the inflammatory response, positive regulation of nitric oxide, biosynthetic process, and positive regulation of ERK1 and ERK2 cascade. The 15 biological processes ranked according to the FDR value are shown in Figure 5(c). We speculate that DHLP may ameliorate RA via complex multichannel synergy.

To further explore the mechanism of action of DHLP in treating RA, we conducted KEGG enrichment analysis on 167 targets and screened out 88 related pathways according to FDR <0.01. After sorting according to the FDR value, the top 15 ranked pathways are shown in Figure 5(d). They include the TNF signalling pathway, hepatitis B, pathways in cancer, Chagas disease (American trypanosomiasis), the toll-like receptor signalling pathway, and other related pathways.

3.2.5. Construction of the TCM-Component-Target-Pathway Network. To clarify the relationship between medicinal materials, ingredients, targets, and pathways, we used Cytoscape 3.7.1 to construct a TCM-component-target-pathway network (Figure 5(e)). Through this network, we can visually demonstrate the effective substances in DHLP that treat RA, as well as their possible mechanisms of action.

4. Discussion

DHLP is a famous TCM that contains a wide variety of medicinal materials. However, DHLP is a complex mixture of a wide variety of herbal medicines, and this composition may cause problems such as difficult drug quality control and the restriction of medicines [38, 39]. UPLC-Q-exactive-orbitrap-MS has high sensitivity and selectivity and is widely used in the analysis of chemical components in complex chemical systems of TCM. Therefore, we used UPLC-Q-exactive-orbitrap-MS in the positive and negative ion modes to quickly identify the chemical components in DHLP and the DHLP components absorbed in blood. According to the retention time, molecular ion peaks, and fragments, as well as the chemical composition of DHLP based on the related literature, we identified 117 compounds in the positive ion mode and 41 compounds in the negative ion mode, including 34 alkaloids, 27 flavonoids, 19 terpenes, 16 glycosides, and 10 phenylpropanoids. Furthermore, we identified 27 prototype components absorbed in blood based on comparison with the *in vitro* ingredients, including 11 flavonoids, 3 glycosides, and 2 alkaloids. This information provides an experimental basis to find new active ingredients of DHLP, to improve quality control standards, and to guide the rational clinical use of drugs.

Network pharmacology is based on biological networks that reveal the interconnections between complex diseases, symptoms, and prescriptions. Many scholars have used this approach to conduct in-depth research on TCM. Based on network pharmacology, we identified 48 compounds, 18 core targets, and 88 related pathways in DHLP that may be related to the treatment of RA. Among them, the top seven core targets are AKT1, MAPK1, STAT3, VEGFA, MAPK8, EGFR, and TNF. MAPK1 is also called ERK2, and a high concentration of epidermal growth factor (EDF) promotes the expression of COX-2 by stimulating the activity of ERK1/2-MAPK to participate in the inflammatory response of RA [40]. TNF participates in the formation of pannus and can promote cartilage destruction and aggravate inflammation to promote the formation and development of RA [41]. Therefore, the chemical components in DHLP may treat RA by regulating related proteins such as MAPK1 and TNF. KEGG enrichment analysis revealed enrichment of osteoclast differentiation and TNF, toll-like receptor, and HIF-1 signalling pathways, among others. Mesenchymal stem cells can directly inhibit osteoclast differentiation by producing NF-κB receptor activator ligands to induce

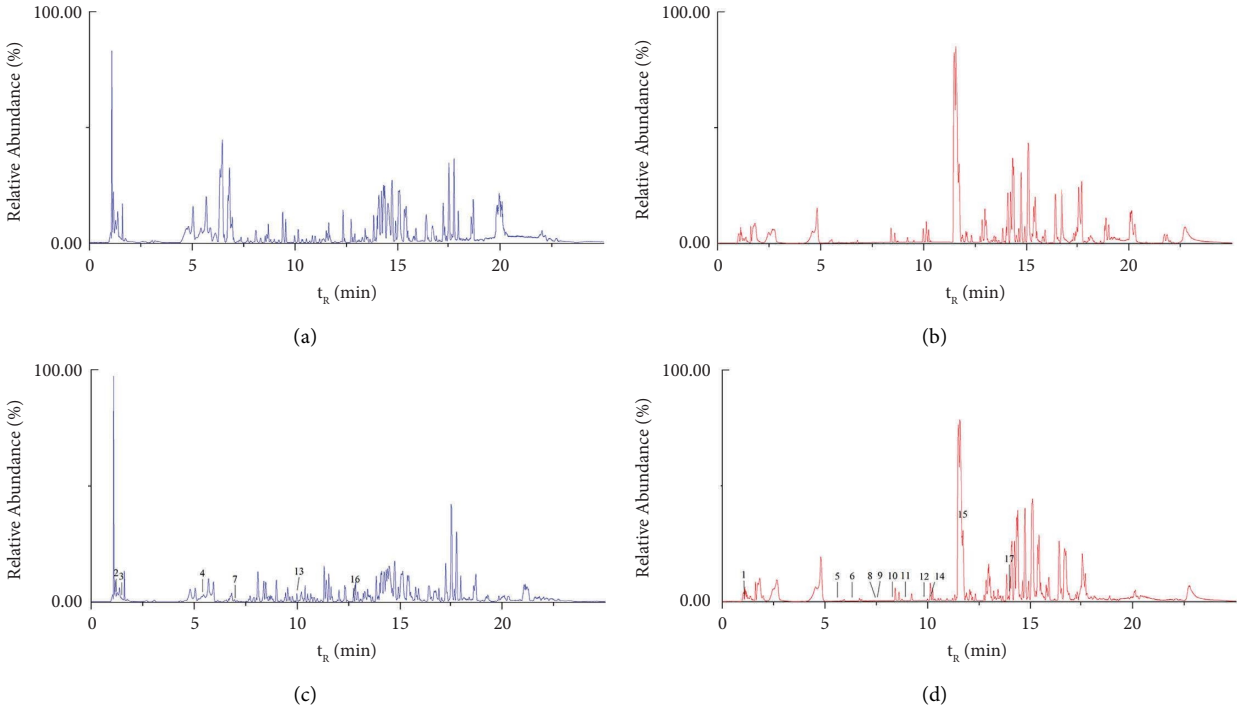

Figure 4: BPI of blank plasma in negative ion (a) and positive ion (b) and plasma samples after administration of DHLP in negative ion (c) and positive ion (d) by UPLC-Q-exactive-orbitrap-MS.

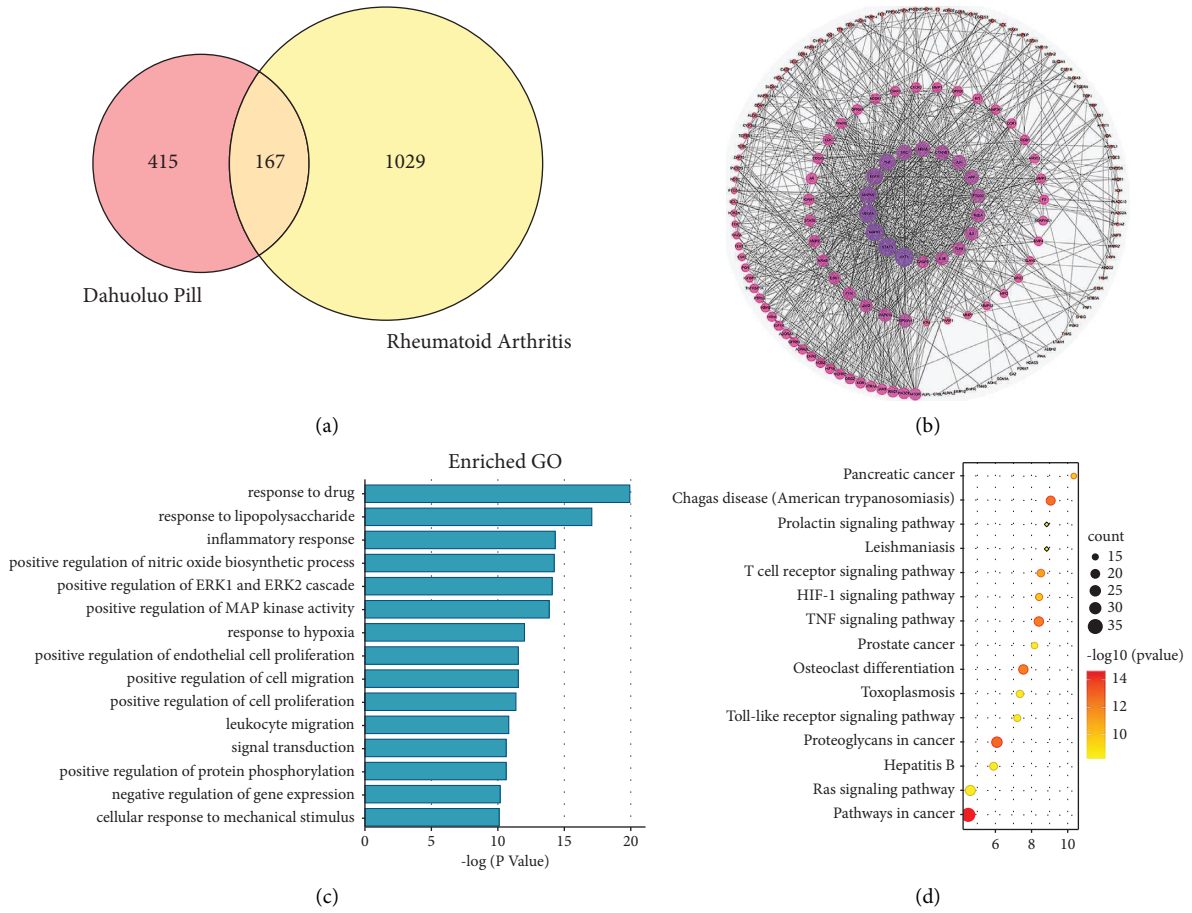

Figure 5: Continued.

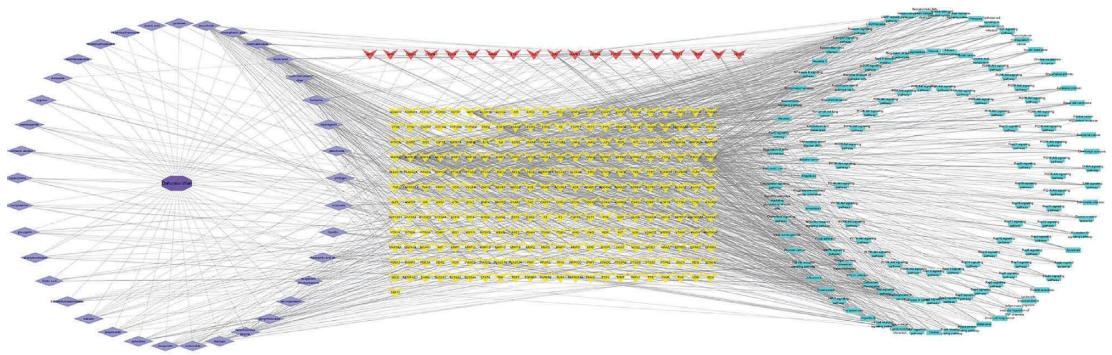

(e)

Figure 5: The Venn diagram of common targets from the components and disease (a) and the PPI network of 167 targets in DHLP (b). The GO enrichment analysis (c) and the KEGG pathways analysis (d) of 167 targets. Traditional Chinese medicine-component-target-pathway network (e).

Table 4: The information of 15 key targets.

Gene name	Target	UniProt ID	Degree
AKT1	Serine/threonine-protein kinase AKT	P31749	52
STAT3	Signal transducer and activator of transcription 3	P40763	50
MAPK1	c-Jun N-terminal kinase 3	P53779	50
VEGFA	Vascular endothelial growth factor A	P15692	48
MAPK8	c-Jun N-terminal kinase 1	P45983	45
EGFR	Epidermal growth factor receptor ErbB1	P00533	44
TNF	TNF-alpha	P01375	43
SRC	Tyrosine-protein kinase SRC	P12931	38
HRAS	Transforming protein p21/H-Ras-1	P01112	36
CTNNB1	Axin1/beta-catenin	P35222	34
JUN	Proto-oncogene c-JUN	P05412	33
APP	Beta-amyloid A4 protein	P05067	33
PTGS2	Cyclooxygenase-2	P35354	31
RELA	Nuclear factor NF-kappa-B p65 subunit	Q04206	30
IL2	Interleukin-2	P60568	29
TLR4	Toll-like receptor 4 (by homology)	O00206	28
IL1B	Interleukin-1 beta	P01584	28
CASP3	Caspase-3	P42574	24

osteoprotegerin production [42]. The toll-like receptor signalling pathway plays an important role in joint destruction caused by chronic expression of proinflammatory cytokines and chemokines [43]. The HIF-1 signalling pathway is an important angiogenesis pathway in RA. HIF-1 affects cell reactivity in synovial tissue under hypoxia to promote the infiltration of macrophages and other inflammatory cells, producing vascular endothelial growth factor (VEGF) and increasing the release of TNF inflammatory mediators, which leads to the persistence of synovitis [44]. Therefore, we speculate that DHLP may ameliorate RA by regulating osteoclast differentiation, by altering the toll-like receptor and HIF-1 signalling pathways, and by acting through other mechanisms.

The prototype components absorbed in blood include glycosmisic acid, costunolide, wogonoside, and chlorogenic acid. Chrysophanic acid could alleviate the pathological changes of osteonecrosis of the femoral head by augmenting osteogenesis and retarding adipogenesis in the scenario of ethanol administration, which may appear during the course of RA [45]. We identified glycosmisic acid, which is found in *Glycyrrhiza uralensis*, as a prototype component and an active ingredient. It exerts anti-inflammatory effects by inhibiting the expression of NF-κB, IL-6, and IL-8 [32]. Wogonoside, which is mainly contained in *Radix scutellariae*, attenuates IL-1β-induced extracellular matrix degradation and hypertrophy in mouse chondrocytes by suppressing activation of NF-κB/HIF-2α in the PI3K/AKT pathway [33] and can also suppress lipopolysaccharide-stimulated production of inflammatory factors by repressing the activation of the JNK/c-Jun signalling pathway in macrophages [36]. The absorbed components mainly ameliorate RA by acting on targets such as STAT3, IL-2, and MMP12 through the toll-like receptor, MAPK, T-cell receptor, and other pathways.

In summary, we employed UPLC-Q-extactive-orbitrap-MS and identified 153 chemical compounds from DHLP and 27 prototype components of DHLP absorbed in

blood, and we explored the potential mechanism for the treatment of RA through the method of network pharmacology. We screened 48 potential active ingredients based on the MS results and the related literature. We identified 1480 potential targets based on these 48 compounds, with 1196 RA-related disease targets, including 167 common targets for DHLP and RA. The GO biological process and KEGG signalling pathway enrichment analysis for these targets predicted that DHLP could regulate MAPK1, STAT3, AKT1, MAPK8, TNF, and other targets and that DHLP could regulate TNF, toll-like receptor, HIF-1, and other signalling pathways as well as osteoclast differentiation to suppress inflammation and to regulate immune function to treat RA. The results of the current study provide important experimental data and bioinformatics analysis for further development and rational use of DHLP.

Data Availability

The data used to support the findings of this study are included within the article.

Disclosure

Haoran Xu and Yuelin Bi are the co-first authors of the article.

Conflicts of Interest

The authors declare that they have no conflicts of interest.

Authors' Contributions

Haoran Xu and Yuelin Bi contributed equally to this manuscript.

Acknowledgments

The financial support was provided by the National Natural Science Foundation of China (NSFC) (Grant no. 81373942), the 2022 Medical and Health Science and Technology Plan of Xiangyang City, Hubei Province (Grant no. 2022YL30A), the Hubei Province Natural Science Foundation (Grant no. 2022CFB867), and the Education Department Foundation of Liaoning Province (Grant no. LZ2020074). The authors are very grateful for the support of the Analysis and Testing Center of Beijing University of Chinese Medicine. Funding was provided for the graduate training of the Beijing University of Traditional Chinese Medicine.

References

[1] Y. J. Lin, M. Anzaghe, and S. Schülke, "Update on the pathomechanism, diagnosis, and treatment options for rheumatoid arthritis," *Cells*, vol. 9, no. 4, p. 880, 2020.

[2] D. Aletaha and J. S. Smolen, "Diagnosis and management of rheumatoid arthritis: a review," *JAMA*, vol. 320, no. 13, pp. 1360–1372, 2018.

[3] J. A. Sparks, "Rheumatoid arthritis," *Annals of Internal Medicine*, vol. 170, no. 1, p. ITC1, 2019.

[4] L. Q. Chi, B. Zhou, W. Y. Gao, and Z. Liu, "Research progress of drugs commonly used to anti-rheumatoid arthritis," *China Journal of Chinese Materia Medica*, vol. 39, no. 15, pp. 2851–2858, 2014.

[5] X. F. Huang, "Study on the effect of Dahuoluo pills in the recovery of neurological function in patients with cerebral infarction," *Journal of Traditional Chinese Medicine*, vol. 26, pp. 677-678, 2014.

[6] L. Z. Shang, J. H. Feng, and S. W. Ren, "Dahuoluo pills combined with pain point injection for treatment of 100 cases of frozen shoulder," *Shaanxi Journal of Traditional Chinese Medicine*, vol. 33, pp. 1014-1015, 2012.

[7] X. W. Zeng and S. G. Li, "Research progress of rheumatoid arthritis therapy and the molecular mechanisms of immunity," *Journal of Chinese Practical Diagnosis and Therapy*, vol. 29, pp. 1044–1046, 2015.

[8] S. B. Xu, H. Xiang, and M. Lu, "The effect of dahuoluo pills in promoting blood circulation and removing blood stasis," *Sun Yatsen University Forum*, pp. 192–195, 1994.

[9] M. L. Yan, L. F. Cong, and Z. Y. Zhang, "Rapid evaluation of anti-inflammatory efficacy of Angelica sinensis(oliv.) diels by near infrared spectroscopy based on quality markers," *Journal of Instrumental Analysis*, vol. 39, pp. 1320–1326, 2020.

[10] Q. X. Yang, *Study on the Chemical Constituents of Cinnamon [master]*, Guangdong Pharm Univ, Guangzhou, China, 2017.

[11] Q. Wang, Z. W. Lu, Y. H. Liu et al., "Rapid analysis on phenolic compounds in Rheum palmatum based on UPLC-Q-TOF/MSE combined with diagnostic ions filter," *China Journal of Chinese Materia Medica*, vol. 42, no. 10, pp. 1922–1931, 2017.

[12] B. F. Jin, H. Ye, and F. Y. Wang, "Chemical component analysis of raw polygoni multiflori Radix by UPLC/Q-TOF MS," *Journal of Guangdong Pharmaceutical University*, vol. 36, pp. 473–478, 2020.

[13] M. R. Zhi, X. R. Gu, S. Han et al., "Chemical variation in aconti kusnezoffii Radix before and after processing based on UPLC-orbitrap-MS," *China Journal of Chinese Materia Medica*, vol. 45, no. 5, pp. 1082–1089, 2020.

[14] Y. J. Sun, Z. P. Huo, and Y. Wang, "Analysis of chemical constituents in jiechangyan qixiao granules based on UPLC-Q-TOF/MSE," *Chinese Journal of Experimental Traditional Medical Formulae*, vol. 27, no. 9, pp. 157–167, 2021.

[15] B. Y. Zhang, Z. Z. Jiang, and Y. F. Wang, "Analysis of chemical constituents in fresh,dried and prepared Rehmanniae Radix by UPLC/ESI-Q-TOF MS," *Chinese Traditional Patent Medicine*, vol. 38, pp. 1104–1108, 2016.

[16] N. Zhang, X. Gao, Y. Zhou et al., "Rapid identification of chemical components in xingbei zhike keli by UPLC-Q-TOF-MS/MS," *China Journal of Chinese Materia Medica*, vol. 43, no. 22, pp. 4439–4449, 2018.

[17] T. T. Wang, R. An, and K. Liang, "Chemical constituent analysis of gegen qinlian decoction based on UPLC-LTQ-orbitrap-MS," *Chinese Traditional and Herbal Drugs*, vol. 51, pp. 1498–1507, 2020.

[18] B. Yang, Y. Wang, and M. Tian, "Analysis on Chemical Constituents of Glycyrrhizae Radix et Rhizoma in Pinelliae Rhizoma Praeparatum by UPLC-Q-TOF-MS/MS," *Chinese Journal of Experimental Traditional Medical Formulae*, vol. 23, pp. 45–49, 2017.

[19] J. H. Zhang, W. D. Wu, and J. T. Liu, "Rapid analysis of chemical constituents of Huoxue Zhitong Capsules based on UPLC-Q-TOF/MS," *Chinese Traditional and Herbal Drugs*, vol. 51, pp. 3139–3146, 2020.

[20] H. Chen, C. Y. Liu, and C. Y. Li, "Advances in studies on chemical constituents and pharmacologic effects of Pericarpium Citri Reticulatae Viride," *Chinese Traditional and Herbal Drugs*, vol. 11, pp. 93–95, 2001.

[21] H. P. Long, X. Li, and T. T. Wang, "Study on chemical constituents from xiaoer fupi granules based on UPLC-LTQ-orbitrap-MS," *Chinese Traditional and Herbal Drugs*, vol. 49, pp. 5522–5531, 2018.

[22] Y. M. Zhong, Y. F. Feng, and J. Guo, "Rapid identification of components fromAtractylodis macrocephalae rhizoma based on UPLC/Q-TOF MS," *Journal of Chinese Mass Spectrometry Society*, vol. 36, pp. 72–77, 2015.

[23] M. J. Liu, Y. Wang, L. Y. Li et al., "UPLC-Q-TOF/MS for rapid analysis of chemical constituents in Sanhuang tablets," *China Journal of Chinese Materia Medica*, vol. 42, no. 9, pp. 1685–1692, 2017.

[24] G. S. Li, Y. Ma, T. Geng et al., "Rapid identification of chemical components in compound Nanxing acesodyne plaster by UPLC-Q-TOF-MS/MS," *China Journal of Chinese Materia Medica*, vol. 44, no. 2, pp. 298–307, 2019.

[25] X. L. Ren, J. H. Huo, and G. D. Sun, "Analysis of chemical components as coumarin in saposhnikovia divaricata by UPLC-Q-TOF-MS," *China Pharmacy*, vol. 30, pp. 349–354, 2019.

[26] Q. Y. J. Zhou, Z. X. Qing, and P. Cai, "Study on substance basis of yinhuang qingfei capsule in vitro by HPLC-Q-TOF-MS/MS," *Chinese Traditional and Herbal Drugs*, vol. 47, pp. 3586–3593, 2016.

[27] D. K. Zhang, X. Han, R. Y. Li et al., "Analysis on characteristic constituents of crude Aconitum carmichaelii in different regions based on UPLC-Q-TOF-MS," *China Journal of Chinese Materia Medica*, vol. 41, no. 3, pp. 463–469, 2016.

[28] D. W. Liu, G. L. Yan, and Y. Fang, "Utility of UPLC-ESI-TOF/MS for rapid analysis of the constituents in scutellariae Radix," *Traditional Chinese medicine Information*, vol. 29, pp. 20–24, 2012.

[29] H. Hong, W. F. Du, and X. J. Kang, "Qualitative comparison of the chemical constituents of the roots and taproots of Lindera aggregate base on UPLC-Triple-TOF/MS," *Journal of Chinese Medicinal Materials*, vol. 43, no. 3, pp. 615–620, 2020.

[30] X. X. Pan, F. Y. Song, and H. Li, "Identification of chemical compositions in chenxiang huaqi pills by UPLC-Q-TOF/MS," *Chinese Traditional and Herbal Drugs*, vol. 49, pp. 2984–2992, 2018.

[31] Y. Shao, Y. P. Yang, and J. Y. Li, "HPLC-Q-TOF-MS/MS analysis of chemical constituents of fangfeng shaoyaotang," *Chinese Journal of Experimental Traditional Medical Formulae*, vol. 24, pp. 54–59, 2018.

[32] Z. Y. Pan, N. W. Chang, and M. G. Zhou, "Screening of activity components with anti-inflammation in Sang Ju Yin and verification of monomer," *Chinese Traditional and Herbal Drugs*, vol. 47, pp. 1289–1296, 2016.

[33] Q. Tang, G. Zheng, Z. H. Feng et al., "Wogonoside inhibits IL-1β induced catabolism and hypertrophy in mouse chondrocyte and ameliorates murine osteoarthritis," *Oncotarget*, vol. 8, no. 37, pp. 61440–61456, 2017.

[34] S. J. Wu and X. X. Yang, "Studies on the chemical constituents of Mianma Guanzhong—II. Mass spectrometry-mass spectrometry analysis of pyrogallol derivatives," *Chinese Traditional and Herbal Drugs*, vol. 12, pp. 712–715, 1997.

[35] B. Feng, H. Z. Huang, and K. P. Xiong, "Identification of chemical constituents in Xiaojin pills based on UPLC-Q-TOF-MS and GC-MS," *Chinese Journal of Hospital Pharmacy*, vol. 39, pp. 929–936, 2019.

[36] X. Yu, D. D. Chen, L. W. Wang et al., "Wogonoside inhibits inflammatory cytokine production in lipopolysaccharide-stimulated macrophage by suppressing the activation of the JNK/c-Jun signaling pathway," *Annals of Translational Medicine*, vol. 8, p. 532, 2020.

[37] H. P. Su and Y. Han, "Chemical constituents from zhongtong film coating by UPLC-Q-TOF-MS/MS," *Chinese Journal of Experimental Traditional Medical Formulae*, vol. 22, pp. 63–70, 2016.

[38] S. Shen, "Disadvantages of large prescription and large dose application of Chinese medicine," *China Pharmacy*, vol. 46, 2006.

[39] Y. Tan, "Analysis on the prescription of traditional Chinese medicine," *Xinjiang Journal of Traditional Chinese Medicine*, vol. 27, pp. 4–6, 2009.

[40] S. S. Nah, H. J. Won, E. Ha et al., "Epidermal growth factor increases prostaglandin E2 production via ERK1/2 MAPK and NF-κB pathway in fibroblast like synoviocytes from patients with rheumatoid arthritis," *Rheumatology International*, vol. 30, no. 4, pp. 443–449, 2010.

[41] H. Shi, D. T. Wang, and R. G. Wu, "Role of tumor necrosis factor-α mediated nuclear factor kappa B signaling pathway in antiogenesis in rheumatoid arthritis," *Medical Recapitulate*, vol. 18, pp. 2397–2400, 2012.

[42] K. Oshita, K. Yamaoka, N. Udagawa et al., "Human mesenchymal stem cells inhibit osteoclastogenesis through osteoprotegerin production," *Arthritis & Rheumatism*, vol. 63, no. 6, pp. 1658–1667, 2011.

[43] Q. Huang and R. M. Pope, "Toll-like receptor signaling: a potential link among rheumatoid arthritis, systemic lupus, and atherosclerosis," *Journal of Leukocyte Biology*, vol. 88, no. 2, pp. 253–262, 2010.

[44] J. Westra, G. Molema, and C. G. Kallenberg, "Hypoxia-inducible factor-1 as regulator of angiogenesis in rheumatoid arthritis-therapeutic implications," *Current Medicinal Chemistry*, vol. 17, no. 3, pp. 254–263, 2010.

[45] H. P. Yu, P. Liu, D. Y. Zhu et al., "Chrysophanic acid shifts the differentiation tendency of BMSCs to prevent alcohol-induced osteonecrosis of the femoral head," *Cell Proliferation*, vol. 53, no. 8, 2020.